

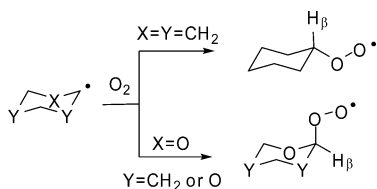
Characterization of Equatorial and Axial Six-Membered-Ring Peroxyl Radicals

Gino A. DiLabio,[†] Keith U. Ingold,[‡] and John C. Walton^{*,§}

National Institute for Nanotechnology, National Research Council of Canada, 11421 Saskatchewan Drive, Edmonton, AB, Canada T6G 2M9, National Research Council, Ottawa, Ontario, Canada K1A 0R6, and University of St. Andrews, School of Chemistry, EaStChem, St. Andrews, Fife KY16 9ST, United Kingdom

jcw@st-and.ac.uk

Received July 5, 2007



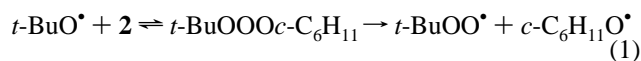
Spectroscopic data are consistent with computations that show that, in their most stable conformations, the peroxy moiety is equatorial in cyclohexylperoxyl radicals and axial in oxa- and most polyoxacyclohexyl-2-peroxyl radicals.

Cyclohexylperoxyl radicals are key propagating species in the industrially important autoxidation of cyclohexane.¹ They, and related oxacyclohexylperoxyl radicals, are capable of existing in equatorial and axial conformations, but no attention has hitherto been given to this phenomenon. Electron paramagnetic resonance (EPR) spectroscopy can distinguish between equatorial and axial cyclohexylcarbinyl radicals ($c\text{-C}_6\text{H}_{11}\text{CH}_2^*$) on the basis of their H_β hyperfine splittings (hfs), a^{H_β} .² The predominant equatorial conformer has a smaller H_β hfs (~ 30 G) than the axial (~ 41 G) because the barrier to rotation about the $C_\beta\text{-C}_\alpha\text{H}_2$ bond is lower for the former radical than for the latter.² Similarly, differences in the magnitudes of a^{H_β} can be used to distinguish conformers of other cycloalk(en)ylcarbinyl radicals (ring sizes up to C_{15}).³ Equatorial and axial cyclohexylacyl radicals ($c\text{-C}_6\text{H}_{11}\text{C}^=\text{O}$) can be differentiated in a similar way.⁴ Cyclohexylperoxyl radicals ($c\text{-C}_6\text{H}_{11}\text{OO}^*$) are known to

have $a^{H_\beta} \approx 5$ G.⁵ In this Note, we report an experimental and theoretical investigation of the equatorial/axial preferences of cyclohexylperoxyl and some oxacyclohexylperoxyls.

Peroxy radicals were generated by UV photolysis of hydrocarbon solutions of cyclohexane and di-*tert*-butyl peroxide (DTBP) under air (Scheme 1). The best resolution was obtained from samples made by distilling cyclopropane onto deaerated cyclohexane (0.03 mL) and DTBP (0.02 mL) in a quartz tube sealed onto the bottom of a larger tube, and then admitting air. The tubes were then flame sealed, thus providing a head space reservoir of air.

The main component of the EPR spectra was a doublet ($a^{H_\beta} = 5.1$ G, $g = 2.0151$, Figure 1a), as previously reported.⁵ However, between this doublet, a singlet was resolved and, when the light was cut off, the doublet decayed rapidly while the singlet showed a brief increase in intensity followed by a much slower decay (Figure 1b,c). The singlet intensity also increased with the duration of photolysis. We attribute this singlet to the relatively persistent *tert*-butylperoxyl radical formed by the known cross-combination/trioxide decomposition of *tert*-butoxyl and alkylperoxyl radicals,^{6,7} eq 1.



The doublet signal was little changed in the temperature range 140 to 220 K, apart from broadening as temperature increased. The oxygen trapping reaction will be extremely fast and diffusion controlled and therefore a 1:1 ratio of **2e** and **2a** might be expected, although the equatorial conformer, **2e**,⁸ will probably predominate for steric reasons. If a significant amount of the axial conformer, **2a**, is present, a^{H_β} (axial) and a^{H_β} (equatorial) must be fairly similar (see below).

It occurred to us that axial cycloalkylperoxyl radicals should predominate if generated from oxacyclohexanes because this conformation would be favored by the anomeric effect. Tetrahydropyran-2-peroxyl, (**3**), 1,4-dioxan-2-peroxyl (**4**), and 1,3,5-trioxan-2-peroxyl (**5**) radicals were therefore generated photochemically under air in cyclopropane, using the corresponding oxacyclohexanes and DTBP. Interestingly, the spectra of peroxyls **3** and **4** were doublets similar to the **2** doublet in the range $140 \text{ K} < T < 215 \text{ K}$ (compare Figure 1a with Figures 1d and 1e).⁹ The spectrum of radical **5** was a singlet, implying a much smaller a^{H_β} in this case (see Figure 1f).¹⁰

(5) (a) Bennett, J. E.; Summers, R. *Trans. Faraday Soc. II* **1973**, 69, 1043. (b) Kemp, T. J.; Welbourn, M. J. *Tetrahedron Lett.* **1974**, 87.

(6) Howard, J. A. *Can. J. Chem.* **1972**, 50, 1981.

(7) To prevent the cross-combination/trioxide decomposition yielding the persistent *t*-BuOO^{*} radical, a cyclopropane solution of cyclohexane and *n*-dodecylperoxide under air was photolyzed at 165 K so that trioxide decomposition would yield the transient primary peroxyl radicals which would be expected to show a poorly resolved 1:2:1 triplet.^{5b} In fact, a very broad singlet was obtained that decayed completely on cutting off the light, leaving no long-lived peroxyl signal. The observed singlet is presumably due to a mixture of cyclohexyl and *n*-alkyl peroxyl radicals, with the lines being broadened by the increased viscosity induced by the dodecyl chains.

(8) Perdeuteriocyclohexylperoxyl radicals generated in a similar way gave, as expected, a singlet, $g = 2.0147$, $a^{D_\beta} \leq 0.9$ G (by simulation).

(9) Note that the shoulders on the high-field components of the spectra in parts d and e of Figure 1 are also due to *t*-BuOO^{*}.

(10) The rapid decay of the singlet in Figure 1f confirmed that it was not the persistent *t*-BuOO^{*}.

[†] NINT, Edmonton.

[‡] NRC, Ottawa.

[§] University of St. Andrews.

(1) (a) Berezin, I. V.; Denisov, E. T.; Emanuel, N. M. *The Oxidation of Cyclohexane*; Pergamon Press: New York, 1996. (b) Schuchardt, U.; Cardoso, D.; Sercheli, R.; Pereira, R.; da Cruz, R. S.; Guerreiro, M. C.; Mandelli, D.; Spinace, E. V.; Pires, E. L. *Appl. Catal. A* **2001**, 211, 1. (c) Hermans, I.; Nguyen, T. L.; Jacobs, P. A.; Peeters, J. *ChemPhysChem* **2005**, 6, 637.

(2) (a) Ingold, K. U.; Walton, J. C. *J. Am. Chem. Soc.* **1985**, 107, 6315.

(b) Ingold, K. U.; Walton, J. C. *J. Chem. Soc., Perkin Trans. II* **1986**, 1337.

(3) Ingold, K. U.; Walton, J. C. *Acc. Chem. Res.* **1989**, 22, 8.

(4) DiLabio, G. A.; Ingold, K. U.; Roydhouse, M. D.; Walton, J. C. *Org. Lett.* **2004**, 6, 4319.

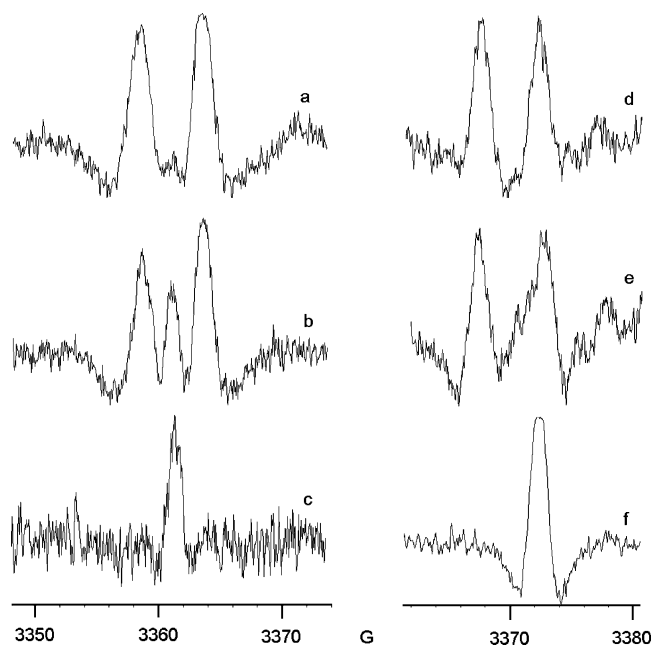


FIGURE 1. Isotropic EPR spectra (second derivatives) of peroxy radicals in cyclopropane: (a) cyclohexylperoxy radicals **2** at 155 K, dark for 0 min, (b) **2** at 155 K, dark for 5 min, (c) **2** at 155 K, dark for 43 min, (d) tetrahydropyranyl-2-peroxy radical **3**, at 145 K, (e) 1,4-dioxanyl-4-peroxy radical **4**, at 155 K, and (f) 1,3,5-trioxanyl-2-peroxy radical **5**, at 200 K.

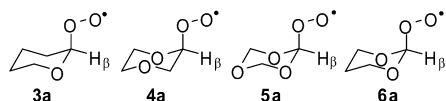
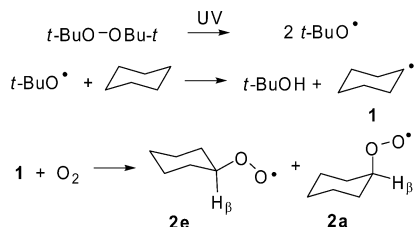


FIGURE 2. Oxacyclohexyl-2-peroxy radicals.¹³

SCHEME 1. Generation of Cyclohexylperoxy Radicals



The semioccupied orbital in the initial tetrahydropyranyl-2-yl radical (and in the analogous C-radicals from which **4–6** were derived) is oriented in an axial direction because of a stabilizing interaction with the lone pair on oxygen. Hence there should be a preference for oxygen entrapment with formation of the axial peroxy radical. Furthermore, by analogy with pyranose sugars, and 2-alkoxytetrahydropyrans,¹¹ the electronegative peroxy substituent is expected to show an axial preference. Thus, conformers **3a** to **6a** (Figure 2) should be stabilized by anomeric effects involving overlap of an axially oriented orbital, associated with the nonbonding electrons of the ring oxygen(s), with a σ^* orbital of the axial exocyclic C–O peroxy bond¹²

(11) Riddell, F. G. *The Conformational Analysis of Heterocyclic Compounds*; Academic Press: New York, 1980.

(12) (a) Thatcher, G. R. *The Anomeric Effect and Associated Stereoelectronic Effects*; Thatcher, G. R., Ed.; American Chemical Society: Washington, DC, 1993. (b) Juaristi, E.; Cuevas, G. *The Anomeric Effect*; CRC Press: Boca Raton, FL, 1995.

(13) The corresponding equatorial radicals are denoted by **3e–6e**. Note that H_β is H_2 in the oxacyclohexa-2-peroxy radicals and H_1 in cyclohexylperoxy radical.

TABLE 1. Isotropic EPR Parameters for Cycloalkylperoxy Radicals in Cyclopropane Solution

radical	T [K]	g -factor	a^{H_β} [G]	
			exptl	computed ^b
2e	155	2.0151	5.1	5.0, 5.0 ^c
2a				5.3 ^c
3e				0.7 ^c
3a	155	2.0160	4.7	4.6, 7.6 ^c
4e				0.4 ^c
4a	155	2.0151	5.3	4.3, 7.9 ^c
5e				1.2 ^c
5a	200	2.0151	$\leq 1^a$	3.1, 3.1 ^c

^a Not resolved; estimated from simulations. ^b Calculated with B3LYP/EPR-III. ^c Computed hfs at the torsional potential minimum.

TABLE 2. Cycloalkylperoxy Computed Energetics (kcal mol⁻¹)

	2e, 2a	3e, 3a	4e, 4a	5e, 5a	6e, 6a
$\Delta E(\text{eq-ax})$	-0.56	1.84	2.12	3.15	3.55
$E^\ddagger[\text{C-O}]^a$	2.3, 3.0	4.3, 2.9	3.9, 2.8	3.9, 2.4	3.8, 2.4

^a Barriers for rotation about the $\text{C}_\beta\text{-OO}^\bullet$ bond.

(see also computational results below). Comparison of the experimental EPR parameters of **3** and **4** with those of **2** (Table 1) suggests that the spectra of axial and equatorial cyclohexylperoxy radicals would be quite similar and unlikely ever to be resolved.

The structures of cycloalkylperoxy radicals **2–6** were computed with use of UB3LYP¹⁴/EPR-III¹⁵ as implemented in the Gaussian-03 package.¹⁶ For **2–6**, the computed $r(\text{O-O})$ values are 1.32 Å. That the anomeric effect is operating in the oxaperoxy radicals is evident from differences in the ring C–O bond lengths: $r(\text{OOC-O})_{\text{axial}}$ values are computed to be 0.01–0.02 Å shorter than the $r(\text{OOC-O})_{\text{equat}}$ values and there is a corresponding lengthening of the ring CO–C bonds of up to 0.01 Å. The differences in energy between the equatorial and axial conformers $\Delta E(\text{eq-ax})$ are shown in Table 2 together with the barriers for rotation about the $\text{C}_\beta\text{-OO}^\bullet$ bond, $E^\ddagger[\text{C-O}]$.

The computed preference for equatorial cyclohexylperoxy radical **2e**, over the axial conformer **2a** is small (0.56 kcal mol⁻¹), implying that an equilibrium mixture would contain minor amounts of **2a** (18.4% at 155 K). The enthalpic preferences for the axial conformers of the 1-oxacyclohexyl-2-peroxy radicals **3a** and **4a** are both much greater (~ 2 kcal mol⁻¹) and in the normal range for the anomeric effects of a RO or HO group.¹⁷ The axial conformers of the 1,3-dioxacyclohexyl-2-peroxy radicals **5a** and **6a**, are computed to be even more stabilized relative to their equatorial conformers (3.15 and 3.55 kcal mol⁻¹).¹⁸ Comparison

(14) (a) Becke, A. D. *J. Chem. Phys.* **1993**, *98*, 5648–5652. (b) Lee, C.; Yang, W.; Parr, R. G. *Phys. Rev. B* **1988**, *37*, 785–789.

(15) Barone, V. In *Recent Advances in Density Functional Theory*; Chong, D. P., Ed.; World Scientific Publishing Co.: Singapore, 1996.

(16) Frisch, M. J.; et al. *Gaussian 03*, revision D.01; Gaussian, Inc.: Pittsburgh, PA, 2003 (see the Supporting Information for full citation).

(17) (a) Lii, J. H.; Chen, K. H.; Durkin, K. A.; Allinger, N. L. *J. Comput. Chem.* **2003**, *24*, 1473. (b) Jones Wheldon, A.; Vickrey, T. L.; Tschumper, G. S. *J. Phys. Chem. A* **2005**, *109*, 11073.

(18) Secondary orbital interactions were examined by Natural Bonding Orbital analyses on the B3LYP/EPR-III wave functions. The equatorial conformations **2e–6e** all showed several stabilizing interactions in the range 2.5 to 6.5 kcal mol⁻¹, generally hyperconjugative in nature. The 1-oxa axial radicals, **3a** and **4a**, showed an additional interaction of ca. 10 kcal mol⁻¹ involving donation from a lone pair orbital on the ring oxygen to an antibonding orbital associated with the peroxy C–O. The 1,3-dioxo axial radicals, **5a** and **6a**, exhibited two interactions of the same magnitude and character.

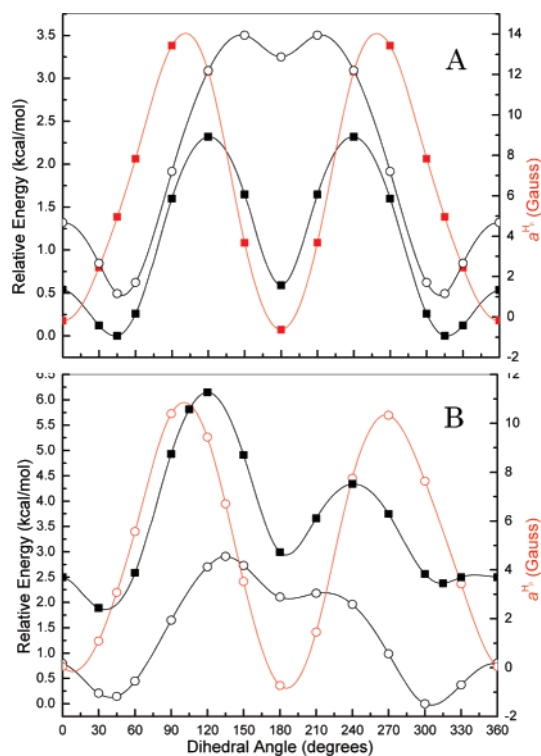


FIGURE 3. Relative energy plots for the rotation about the OO–CH β bond diedral angles and (in red) $a^{\text{H}\beta}$ vs θ plots for **2e** and **3a**: (A) **2a** (○) and **2e** (■) and (B) **3a** (○) and **3e** (■). The plots are offset by the conformer energy difference at their respective minima.

of the experimental and computed $a^{\text{H}\beta}$ values indicates that for **3** and **4** the axial conformers are likely to be dominant, but that this may not be true for **5**.

The potential energy (PE) profiles for rotation of the peroxy groups about the C β –O bond were obtained by incrementing the diedral angle while allowing all of the other degrees of freedom in the radical to relax.

The PE plots for the equatorial radicals, **2e**–**6e**, are all rather similar with triple minima, two main minima (equal in energy for the symmetric **2e**, **5e**, and **6e**) having H β COO diedral angles, θ , of about 45° and 315°, together with a less pronounced secondary minimum at $\theta = 180^\circ$. The PE plots for **2a**–**6a** are also rather similar with two main minima (again equal in energy for the symmetric **2a**, **5a**, and **6a**) having $\theta \approx 45^\circ$ and 315°, together with very shallow minima at 180°. Figure 3 shows representative PE plots for **2a**, **2e** and **3a**, **3e** plus $a^{\text{H}\beta}$ vs θ plots for the major conformers (see the Supporting Information for plots of **4**, **5**, and **6**).

The computed rotational barriers for both the axial and equatorial peroxy radicals, **2**–**6** (Table 2), are considerably higher than those found previously for axial and equatorial $c\text{-C}_6\text{H}_{11}\text{CH}_2^\bullet$, viz.,^{2,3} 1.1 and 0.3 kcal mol $^{-1}$, respectively. This can be attributed only in part to the greater steric bulk of –OO $^\bullet$ compared with –CH $_2^\bullet$ because the rotation barriers for the equatorial 1,3-dioxacyclohexyl-2-peroxy radicals, **5e** and **6e**, are so much greater than that for **2e** despite the fact that in **5e** and **6e** the –OO $^\bullet$ moiety rotates past O $_1$ rather than past the larger CH $_2$ group as in **2e**. We attribute the higher rotation barriers for **5e** and **6e** compared with **2e** to dipole–dipole repulsion between –O $^{\delta+}$ –O $^{\delta-}$ and –C $_2^{\delta+}$ –O $_1^{\delta-}$ in the **5e** and **6e** rings. Rotation barriers for all the axial oxacyclohexyl radicals, **2a**–**6a**, are similar (Table 2). This is because these barriers arise from steric

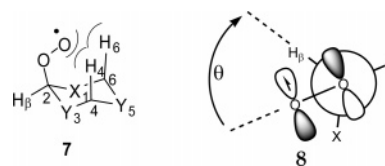


FIGURE 4. Structure **7** shows the hindrance from axial H-atoms. **8** shows a Newman projection of oxacyclohexylperoxy radicals illustrating the antibonding, π -type singly occupied MO.

SCHEME 2. Termination of Cycloalkylperoxy Radicals



interactions with the axial H-atoms on C $_{4,6}$ (see **7** in Figure 4). For **2a** the minimum separation between O $^\bullet$ and H $_{4,6}$ is 2.52 Å and occurs when $\theta \approx 150^\circ$ and 210°, Figure 3A. For **3a** the minimum O $^\bullet$ –H $_{4,6}$ separation involves the axial H $_6$ on C $_6$ (i.e., the C-atom adjacent to the ring O) and is only 2.31 Å and occurs when $\theta \approx 135^\circ$ (Figure 3B), rather than 150°, because of distortion of the regular chair structure by the ring O. This barrier is slightly higher than the barrier due to the axial H $_4$ on C $_4$ for which the minimum O $^\bullet$ –H $_4$ separation is 2.55 Å and occurs when $\theta \approx 210^\circ$ (Figure 3B).

The unpaired electron in peroxy radicals resides in a π -orbital lying above and below the C $_2$ –OO $^\bullet$ plane (see **8** in Figure 4). When the O–O $^\bullet$ and C $_2$ –H bonds are eclipsed, i.e., when $\theta = 0^\circ$ (as drawn in the structures shown in Scheme 1 and Figure 2), $a^{\text{H}\beta}$ will be close to zero, and it will be maximized when $\theta = 90^\circ$, see $a^{\text{H}\beta}$ vs θ plots in Figure 3 and the Supporting Information. Assuming several rotational states exist in each minimum, average $a^{\text{H}\beta}$ values were derived for **2e**, **3a**, **4a**, and **5a** and are shown in Table 1, together with the computed values at the potential minima.¹⁹ There is generally very satisfactory agreement in H β hfs between experiment and theory. Interestingly, the computed H β hfs for **2a** and **2e** are very similar (implying similar average θ values and accounting for the failure to resolve **2a** despite its presumed formation, see above), but for **3**, **4**, and **5** the H β hfs for the axial conformers are larger than those for the equatorial (indicating that average θ values are considerably larger for the axial conformers).

EPR spectra of three crown ether peroxy radicals were also obtained by photolyses of DTBP and the ether in *tert*-butylbenzene at 220 K under air. Doublets ($g = 2.015$) were obtained in each case and values of $a^{\text{H}\beta}/\text{G}$ were 3.0, 1.8, and ~ 1.6 (incompletely resolved) for the peroxy radicals from 12-crown-4, 15-crown-5, and 18-crown-6, respectively. It seems probable that these peroxy radicals were present mainly in pseudoaxial conformations.

Finally, the decays of two of the peroxy radicals were monitored at 155 K on cutting off the light. Decay of **2** occurred with second-order kinetics and, by analogy with other secondary alkyl peroxy radicals, presumably yields the corresponding alcohol and ketone plus O $_2$ (Scheme 2).

The rate constants for the bimolecular self-reactions of **2**–(**a**+**e**) and **3a** were estimated to be 1.3×10^4 and $\geq 10^6$ M $^{-1}$ s $^{-1}$, respectively (for details see the Supporting Information). We hypothesize that this rather large difference in rate constants is less likely to be due to the conformational preferences of these two peroxy radicals than to the expected weaker C $_2$ –H β bond in **3a** (two O atoms attached to C $_2$) than in **2**–(**a**+**e**) (one O atom

(19) See the Supporting Information for the averaging method.

attached to C₂), which should facilitate the transfer of H_β between two **3a** peroxy radicals relative to its transfer between two **2(a+e)** peroxy radicals.

The EPR spectra of equatorial/axial cyclohexylperoxy radicals and oxacyclohexyl-2-peroxy radicals were found to be rather similar, even though calculations indicate that the latter probably have axial conformations, a consequence of the anomeric effect. Evidence for the importance of dipole–dipole repulsion between the exocyclic –O–O• and the ring –C₂–O₁ was uncovered.

Experimental Section

Materials. Cyclohexane, the oxacyclohexanes, and the crown ethers were commercial products used as supplied. Di-*tert*-butyl peroxide was passed down a column of neutral alumina and distilled under reduced pressure. Didodecyl peroxide was prepared from dodecyl bromide and potassium superoxide in the presence of dibenzo-18-crown-6 according to the method of Foglia et al.,²⁰ except that trifluorotoluene was used as solvent. It was then purified by column chromatography on silica gel with cyclohexane as eluant. ¹H NMR (300 MHz, CDCl₃) δ_H 0.88 (6H, t, *J* = 7 Hz), 1.5 (40H, br s), 4.00 (4H, t, *J* = 7 Hz).

Spectra. EPR spectra were obtained with a spectrometer operating at 9.5 GHz with 100 kHz modulation. Solutions were made by distilling cyclopropane (ca. 0.5 mL) onto the deaerated cycloalkane (0.03 mL) and DTBP (0.02 mL) in a quartz tube (0.4 × 12 cm) sealed onto the bottom of a larger tube (0.5 × 25 cm), and then admitting air (ca. 500 mmHg). The tubes were then flame

sealed, thus providing a head space as a reservoir of air. Most of the radicals were also observed at higher temperatures with *tert*-butylbenzene as solvent. Samples were irradiated in the resonant cavity by unfiltered light from a 500 W super pressure Hg arc. Hfs were assigned with the aid of computer simulations, using the Bruker SimFonia software package. Peroxy radical concentrations were determined by double and triple integration of the total signal, using the Bruker WinEPR software and comparison with that of DPPH (1.0 × 10⁻³ M in toluene).

Computational Methods. Quantum chemical calculations were carried out with the Gaussian 03 package.¹⁶ The equilibrium geometries were fully optimized and thermodynamic properties were computed with B3LYP/EPR-III as described in the text. Zero-point vibrational energies and thermal corrections to 298 K were evaluated. Isotropic EPR hfs were derived from computed Fermi contact integrals evaluated at the H-nuclei. The hfs were taken directly from the Gaussian output files.

Acknowledgment. We thank EaStChem, Westgrid and the Center of Excellence in Integrated Nanotools (University of Alberta) for support of this work. We also thank Dr. Peter Mulder for some very helpful comments on an earlier version of this manuscript.

Supporting Information Available: Experimental and computational details, quantitative data for the decay of singlet and doublet peroxy radicals, and EPR spectra for **2e** generated with didodecyl peroxide. This material is available free of charge via the Internet at <http://pubs.acs.org>.

(20) Foglia, T. A.; Silbert, L. *Synthesis* **1992**, 545.